ASEAN Engineering Journal

Full Paper

DEVELOPMENT OF A REHABILITATION ROBOT: MODELING AND TRAJECTORY TRACKING CONTROL

Minh-Chien Trinh, Trong-Hieu Do, Quy-Thinh Dao*

School of Electrical and Electronic Engineering, Hanoi University of Science and Technology, Hanoi, Vietnam

Article history
Received
19 June 2021
Received in revised form
26 December 2021
Accepted
05 February 2022
Published online
30 November 2022

*Corresponding author
thinh.daoquy@hust.edu.vn

Graphical abstract

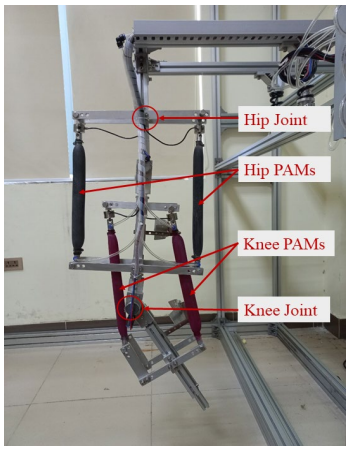

Abstract

Recently, assistive robots have attracted great attention from researchers in the rehabilitation field. These types of robots support patients to perform designated movements during a training process. Despite the existence of commercial rehabilitation systems, growing demands for improvement in both hardware and control design are evident. Therefore, this paper introduces a prototype pneumatic artificial muscle-based assistive robot named BK-Gait and its control strategy for trajectory tracking purposes. Firstly, a brief description of the robot mechanism is presented. Secondly, the mathematical model of the robot's actuator is built. Third, an active disturbance rejection control (ADRC) strategy is developed to enhance the tracking performance of the robot. Finally, multi scenarios experiments are carried out to evaluate the applicability of the robot and the proposed controller in the rehabilitation field.

Keywords: Pneumatic artificial muscle, Active disturbance rejection control, Rehabilitation robot, Extended state observer, Gait training device.

1.0 INTRODUCTION

In rehabilitation, physiotherapists would assist their patients through exercises. The repetition of this work makes them laborious and ineffective. Furthermore, there is no scientific monitoring and analysis of the patient's recovery. Assistive robots are of particular interest in overcoming the above problems as they are designed for a goal-oriented mission, long-term work, and create comfort. Most commercial gait training systems are driven by electric motors. However, these systems show some major concerns related to high costs and the low power/weight ratio of motorized actuators. Therefore, the PAM-based system has been promising for these types of robots because of the following advantages: large power/weight ratio, cost-effectively, lightweight, and similar characteristics to human muscles [1]. Most of the existing PAM-based prototypes have only been developed in research centers [2-5]. From the point of view of the control method, two essential requirements for rehabilitation systems are trajectory tracking control and impedance control. The robot orthosis must provide a needed assist force for guiding the patient's limb to follow the designated trajectory. Besides, it is essential for the patient to feel comfortable during the training session, which is the reason why the robot must have high enough compliance.

Many control methods have been deployed for the artificial muscle system for trajectory tracking purposes. The first choice is the proportional integral derivative (PID) controller and its modified versions [6-7]. However, the difficulty in tuning controller parameters and the inability to adapt to the changes in system parameters makes the PID ineffective in this case. An adaptive controller is proposed to control the upper limb joints in [8], and we find a limitation in this approach with the long computation time and large storage memory. Lilly and Yang applied a sliding control algorithm to the elbow [9], this controller ensures accuracy when there is noise from the model, but the control signal inevitably fluctuates when the system operates near the sliding surface. To improve this, a sliding controller is combined with neural networks to eliminate interference in the control signal [10]. However, using a neural network for approximation can decrease controller performance unless the number of neural and learning time is long enough. In addition, some other studies show pretty positive results [11-13], a typical impedance control function implemented in some

systems [14]. In those systems, the exoskeletal robots can estimate the disability level of patients and provide the needed assistance torques.

Recently in the literature, the linear model has been employed to describe the characteristic of PAMs. In these studies [15-21], the model parameters are obtained with acceptable accuracy. Besides, the uncertain nonlinearity of PAM can be estimated by an extended state observer (ESO) and solved by an active disturbance rejection controller (ADRC). The ADRC method [21] is a controller capable of estimating and eliminating system disturbances, including external noise on the system and non-parametric components. Control rules are based on errors rather than models and are not necessarily dependent on the complete information of the model. With the ADRC, the control performance of these systems is improved and able to track 0.5 Hz sinusoidal signal. However, these researches focus only on the PAMs in antagonistic configuration and do not consider the overall exoskeleton robot proposed in this research.

In this article, we develop a 2-DOF PAM-based prototype robot for lower-limb rehabilitation named BK-Gait. This exoskeletal robot covers the hip and knee joints of the limb. In order to satisfy the trajectory tracking requirement of rehabilitation devices, an ADRC is employed in the system based on the advantages mentioned above. The proposed controller achieves good performance when tracking human gait pattern trajectory.

The rest of the contents are arranged in the following order. First, the system description section presents the robot configuration together with its components. After that, the dynamic behavior of the robot is carefully investigated and described by a discrete-time linear mathematical model. In the next section, the ADRC control algorithm is implemented for trajectory tracking purposes. And finally, the proposed mathematical model and control strategy are both tested and verified by experimental results.

2.0 SYSTEM DESCRIPTIONS

The prototype exoskeletal robot is designed as a 2-DOF robot in Figure 1a. The robot covers the thigh and shank segment of subjects and can be adjusted according to the subjects' body by the slider and fixed by the screw when training. The maximum absolute value of angles of hip and knee joints in flexion/extension movements are 450 and 900, respectively. The robot's main bone is mainly produced from preshaped aluminum. The robot drives the subject's lower limb with two aluminum braces at the thigh and shank parts. Figure 1b presents the actual image of the developed robotic exoskeleton.

Table 1 Length and Nominal Pressure of Robot PAMs.

Robot Joint	Nominal Length [cm]		Nominal Pressure [MPa]	
	Anterior	Posterior	Anterior	Posterior
Hip joint	34	34	0.2	0.2
Knee joint	35	30	0.35	0.2

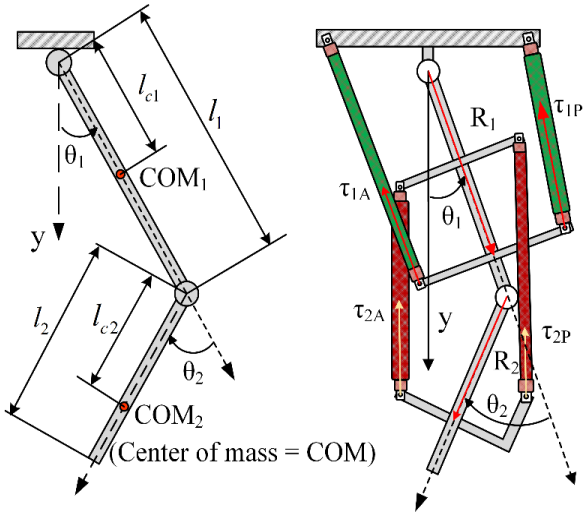

(a)

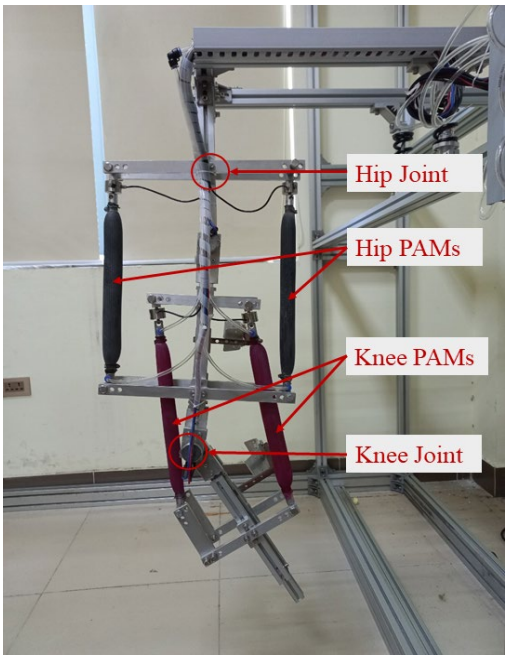

(b)

Figure 1 Proposed lower limb rehabilitation robot: (a) typical 2DOFs robot and (b) actual image of the BK-Gait robot.

The robot is powered by four PAMs. Each PAMs have a diameter of 1.0 inch and can stretch up to 30%. The parameters of the used muscles are provided in Table 1. The proportional control valve ITV1030-04N2CL5 is used to regulate the pressure of the muscles. When there is an air pressure difference between two muscles, two forces will be formed to act on both muscles in two different directions. This will cause one muscle to contract and the other to stretch, causing the mechanism to rotate at a corresponding angle. The rotation angle is measured with a WDD35D4 angle sensor attached to each joint. One end of the muscle tube is connected to a load cell sensor to determine the pulling force of each muscle. A NI MyRIO-1900 platform is used to implement control algorithms which is programmed via LabVIEW software. During the experiment, all the signals obtained from the potentiometers, load cell amplification, and control commands are sent to the NI MyRIO-1900 processing kit through analog input/output channels.

3.0 MATHEMATICAL MODEL OF THE PAM-BASED ROBOT

3.1 Dynamic Model of An Antagonistic Configuration of PAMs

For rehabilitation application, the range of the hip joint is set not to exceed 20°. The knee joint of the BK-Gait exoskeleton robot is designed with L-shape to optimize its movement. For these reasons, we can assume that the rod mechanism of PAM in the BK-Gait design is equivalent to the pulley setup, as shown in Figure 2. The deviation in the mechanism model will be observed and solved by an ESO. In the antagonistic configuration, the initial angle is set to 0° by supplying a fixed amount of pressure to both PAMs. The rotation angle θ can be deflected by the difference in pressure inside each PAMs.

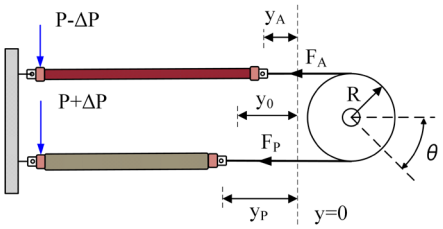

Figure 2. An antagonistic setup of two PAMs.

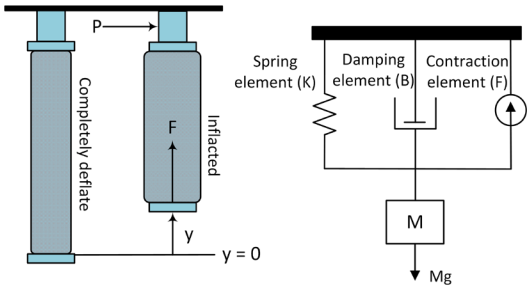

Figure 3. Working principle of a PAM (a) and its three-element model (b).

The muscle's input pressure is expressed as follows:

$$\begin{cases} P_P = P_0 + P' + \Delta P \\ P_A = P_0 - \Delta P \end{cases} \quad (1)$$

where and P_P are the pressure of the anterior and posterior muscles. P_0 and $P_0 + P'$ are the constant pressures that determine the initial lengths of the anterior and posterior muscles. Different pressure ΔP is chosen as the control variable. The length of the muscles are determined as follows:

$$y_{P,A} = y_0 \pm R\theta \quad (2)$$

where y_0 is the initial muscle contraction at pressure P_0 from its complete deflation state.

In order to build the mathematical model of antagonistic configuration, the dynamic behavior of a single pneumatic artificial muscle – mass system will be considered first. In this paper Reynolds's model [1] is employed to describe the single PAMs-mass system's characteristic. The equation describing the displacement y of a mass M hanged by PAM (Figure 3) is:

$$M\ddot{y} + B(P)\dot{y} + K(P)y = F - Mg \quad (3)$$

where

$$\begin{cases} K(P) = K_0 + K_1 P \\ B(P) = B_{0j} + B_{1j} P \\ F(P) = F_0 + F_1 P \end{cases} \quad (4)$$

in which K, B, F are the spring, damping, and contractile force coefficients of the model; K_i , B_{ij} , and F_i with i=1,2 are identified components; j=1,2 represent the contraction and deflation state of PAM. P is the pressure inside the PAM.
In general, the total force generated by the PAM is:

$$F^{PAM} = F(P) - B(P)\ddot{y} - K(P)\dot{y} \quad (5)$$

In the antagonistic configuration of PAMs in this research, the two muscles are initially compressed by supplying the same pressure. This allows us to determine the initial position of the joint. When the input pressure is increased at one muscle, the input pressure in the other muscle is decreased, and vice versa creates a torque T acting on the joint. The dynamic equation of the system is:

$$T = \left(F_A^{PAM} - F_P^{PAM}\right) R \quad (6)$$

From equations (1), (2), (5) and (6), after some transformation, we have:

$$T = T_0 \Delta P + T_1 \dot{\theta} + T_2 \theta + T_3 \quad (7)$$

in which:

$$\begin{cases} T_0 = (2F_1 - 2K_1\theta)R \\ T_1 = -(2B_0 + 2B_1 P_0 + B_1 P')R^2 \\ T_2 = -(2K_0 + 2K_1 P_0 + K_1 P')R^2 \\ T_3 = (F_1 P' - K_1 P' L_0)R \end{cases} \quad (8)$$

3.2 Mathematical Model of 2-DOF Robot Actuated by PAMs

Generally, the dynamic behavior of 2-DOF robot is described by Euler-Lagrange equation:

$$T = M(\theta)\ddot{\theta} + H(\theta)\dot{\theta} + G(\theta) \quad (9)$$

where $\theta = \begin{bmatrix} \theta_1 \\ \theta_2 \end{bmatrix}$ is the robot joint matrix, M is the effective moment of inertia matrix, H is the matrix of viscous moment and radial force, G is the gravity torque matrix, T is the total torque acting on the rotating joint. From equation (7) and equation (9):

$$M(\theta)\ddot{\theta} + H(\theta)\dot{\theta} + G(\theta) = T_0 \Delta P + T_1 \dot{\theta} + T_2 \theta + T_3 \quad (10)$$

Transforming the equation (10) we get:

$$\ddot{\theta} = M^{-1}(-H'\dot{\theta} - G') + M^{-1}T_0\Delta P \tag{11}$$

Where:

$$H' = H - T_1,\ G' = G - T_2\theta - T_3,\ T_0 = \begin{bmatrix} T_{01} & 0 \\ 0 & T_{02} \end{bmatrix} \tag{12}$$

In which T_{0i} and ΔP_i with i = 1, 2 is the T_0 fraction and the differential pressure between the artificial muscles of the hip and knee joints.

4.0 CONTROLLER DESIGN

4.1 ADRC Concept

First, we consider the following second-order system:

$$\ddot{y}(t) = f(t) + b_0 u(t) \tag{13}$$

in which y is the measured output, *u* is the control signal, and $f(t)$ represents the unknown components of the system. Following [20], the generalized term $f(t)$ can be taken into account as a total disturbance. Therefore an Extended State Observer (ESO) is constructed to provide the real-time estimation of $f(t)$, denoted $\hat{f}(t)$. Then the impact of $f(t)$ in the equation (13) can be suppressed by estimated disturbance with the control law is obtained as the following equation:

$$u = \frac{u_0 - \hat{f}}{b_0} \tag{14}$$

Reduces the system in (13) to the form of:

$$\ddot{y} \cong u_0 \tag{15}$$

The system will become easier to control with a simple proportional controller. In general, this concept requires little knowledge of the plant. The only thing required is knowledge of the order of the plant and the approximate value of the parameter b_0. A practical tuning method for a linear ESO was proposed in [21], which helps engineers have an easy-to-understand view and implement the controller. Expressing equation (13) as state space with $x_1 = y,\quad x_2 = \dot{y},\quad x_3 = f,\quad x(t) = \begin{bmatrix} x_1 & x_2 & x_3 \end{bmatrix}^T$ and $\dot{x}(t) = \begin{bmatrix} \dot{x}_1 & \dot{x}_2 & \dot{x}_3 \end{bmatrix}^T$ we have:

$$\dot{x}(t) = Ax(t) + Bu(t) + C\dot{f}(t) \tag{16}$$

where $A = \begin{bmatrix} 0 & 1 & 0 \\ 0 & 0 & 1 \\ 0 & 0 & 0 \end{bmatrix}, B = \begin{bmatrix} 0 \\ b_0 \\ 0 \end{bmatrix}, C = \begin{bmatrix} 0 \\ 0 \\ 1 \end{bmatrix}$, and $\dot{f}(t)$ is the derivative of $f(t)$. The unknown component $f(t)$ cannot be directly measured. However, its estimation can be obtained from *u(t)* and *y(t)* by the following state observer:

$$\begin{aligned} \begin{bmatrix} \dot{z}_1(t) \\ \dot{z}_2(t) \\ \dot{z}_3(t) \end{bmatrix} &= \begin{bmatrix} 0 & 1 & 0 \\ 0 & 0 & 1 \\ 0 & 0 & 0 \end{bmatrix}\begin{bmatrix} z_1(t) \\ z_2(t) \\ z_3(t) \end{bmatrix} + \begin{bmatrix} 0 \\ b_0 \\ 0 \end{bmatrix}u + \begin{bmatrix} l_1 \\ l_2 \\ l_3 \end{bmatrix}(y(t) - z_1(t)) \\ &= \begin{bmatrix} -l_1 & 1 & 0 \\ -l_2 & 0 & 1 \\ -l_3 & 0 & 0 \end{bmatrix}\begin{bmatrix} z_1(t) \\ z_2(t) \\ z_3(t) \end{bmatrix} + \begin{bmatrix} 0 \\ b_0 \\ 0 \end{bmatrix}u + \begin{bmatrix} l_1 \\ l_2 \\ l_3 \end{bmatrix}y(t) \end{aligned} \tag{17}$$

where z_i with $i = 1, 2, 3$ are observed variables, l_i with $i = 1, 2, 3$ are parameters of the ESO to be determined such that z_1, z_2 and z_3 will track $y, \dot{y}, \text{and} f$, respectively. Then the control signal is chosen as:

$$u = \frac{\left[K_P(r - z_1) - K_D z_2\right] - z_3}{b_0} \tag{18}$$

with K_P, K_D are parameters of the controller to be determined. Reduces equation (13) to:

$$\ddot{y} \cong K_P(y^* - y) - K_D\dot{y} \tag{19}$$

In which y^* is the set point. Taking the Laplace transform of (19), one gets:

$$\frac{Y(s)}{Y^*(s)} = \frac{K_P}{s^2 + K_D s + K_P} \tag{20}$$

4.2 ADRC Design for a 2-DOFs PAM-based Robot

According to the above idea, the ADRC can be applied to the PAM-based robot model in equation (11). The nonlinear and uncertainty components of the artificial muscle and the robot model will be considered as disturbance *f*:

$$\begin{bmatrix} \ddot{\theta}_1 \\ \ddot{\theta}_2 \end{bmatrix} = \begin{bmatrix} f_1 \\ f_2 \end{bmatrix} + \begin{bmatrix} b_{01} & 0 \\ 0 & b_{02} \end{bmatrix}\begin{bmatrix} \Delta P_1 \\ \Delta P_2 \end{bmatrix} \tag{21}$$

We have

$$\begin{cases} \begin{bmatrix} f_1 \\ f_2 \end{bmatrix} = M^{-1}(-H'\dot{\theta} - G') + \begin{bmatrix} \Delta b_{11} & \Delta b_{21} \\ \Delta b_{12} & \Delta b_{22} \end{bmatrix}\begin{bmatrix} \Delta P_1 \\ \Delta P_2 \end{bmatrix} \\ M^{-1}T_0\Delta P = \begin{bmatrix} \Delta b_{11} + b_{01} & \Delta b_{21} \\ \Delta b_{12} & \Delta b_{21} + b_{02} \end{bmatrix}\begin{bmatrix} \Delta P_1 \\ \Delta P_2 \end{bmatrix} \end{cases} \tag{22}$$

where Δb_{ij} with *i,j = 1,2* represents the effect of the i^{th} joint's control signal on the i^{th} joints. The control law is selected as follows:

$$\begin{bmatrix} \Delta P_1 \\ \Delta P_2 \end{bmatrix} = \begin{bmatrix} \frac{1}{b_{01}} & 0 \\ 0 & \frac{1}{b_{02}} \end{bmatrix}\left(u_0 - \begin{bmatrix} z_{31} \\ z_{32} \end{bmatrix}\right) \tag{23}$$

where

$$u_0 = \begin{bmatrix} K_{P1}(r_1 - \theta_1) - K_{D1} z_{21} \\ K_{P2}(r_2 - \theta_2) - K_{D2} z_{22} \end{bmatrix} \quad (24)$$

If the two observers work well, substituting equations (23) and (24) into equation (25) will yield:

$$\begin{bmatrix} \ddot{\theta}_1 \\ \ddot{\theta}_2 \end{bmatrix} = \begin{bmatrix} f_1 \\ f_2 \end{bmatrix} - \begin{bmatrix} z_{31} \\ z_{32} \end{bmatrix} + u_0 = \begin{bmatrix} K_{P1}(r_1 - \theta_1) - K_{D1}\dot{\theta}_1 \\ K_{P2}(r_2 - \theta_2) - K_{D2}\dot{\theta}_2 \end{bmatrix} \quad (25)$$

The ADRC structure for the rehabilitation robot is proposed in Figure 4. In that Figure z_{ij} with $i = 1, 2, 3$ and $j = 1, 2$ are observed variables of the i^{th} joint.

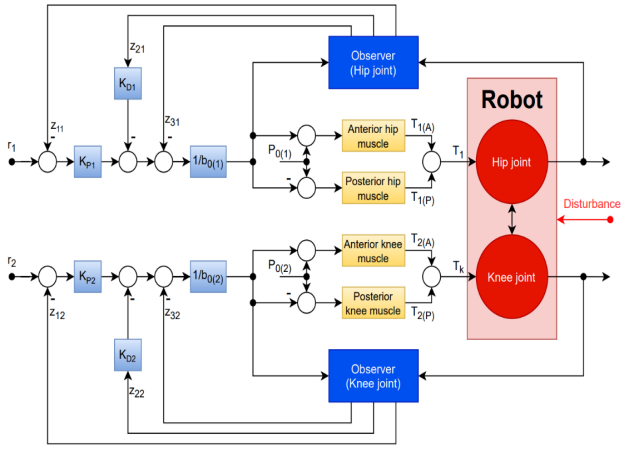

Figure 4. ADRC controller structure of BK-Gait robot.

A tuning method for the parameter of ADRC is presented in [22], which is related to the desired 2% setting time $T_{set}^{2\%}$:

$$\begin{bmatrix} K_{P1} \\ K_{P2} \end{bmatrix} = \begin{bmatrix} \left(s_1^{CL}\right)^2 \\ \left(s_2^{CL}\right)^2 \end{bmatrix}; \begin{bmatrix} K_{D1} \\ K_{D2} \end{bmatrix} = \begin{bmatrix} -2s_1^{CL} \\ -2s_2^{CL} \end{bmatrix}; \begin{bmatrix} s_1^{CL} \\ s_2^{CL} \end{bmatrix} \approx \begin{bmatrix} \dfrac{-6}{T_{set(1)}^{2\%}} \\ \dfrac{-6}{T_{set(2)}^{2\%}} \end{bmatrix} \quad (26)$$

Where s_1^{CL} (respectively s_2^{CL}) is the negative-real double pole of equation (20) for the hip joint (respectively knee joint). The pole of the ESO observer is recommended choosing as follows:

$$\begin{bmatrix} s_1^{ESO} \\ s_2^{ESO} \end{bmatrix} \approx \begin{bmatrix} (3 \ldots 10)\, s_1^{CL} \\ (3 \ldots 10)\, s_2^{CL} \end{bmatrix} \quad (27)$$

We can find the parameters of observers based on the bandwidth parameterization method. The error dynamics of the observer is determined by the matrix (A−LC). By placing all observer poles at one location, the parameters of the observer are obtained as follows:

$$\begin{aligned} \det\left(sI - (A - LC)\right) &= s^3 + l_1 s^2 + l_2 s + l_3 = \left(s - s^{ESO}\right)^3 \\ &= s^3 - 3s^{ESO} s^2 + 3\left(s^{ESO}\right)^2 s - \left(s^{ESO}\right)^3 \end{aligned} \quad (28)$$

By balancing the coefficients of the equation, we can easily obtain:

$$\begin{bmatrix} l_{11} \\ l_{12} \end{bmatrix} = \begin{bmatrix} -3s_1^{ESO} \\ -3s_2^{ESO} \end{bmatrix}; \begin{bmatrix} l_{21} \\ l_{22} \end{bmatrix} = \begin{bmatrix} 3\left(s_1^{ESO}\right)^2 \\ 3\left(s_2^{ESO}\right)^2 \end{bmatrix}; \begin{bmatrix} l_{31} \\ l_{32} \end{bmatrix} = \begin{bmatrix} -\left(s_1^{ESO}\right)^3 \\ -\left(s_2^{ESO}\right)^3 \end{bmatrix} \quad (29)$$

5.0 EXPERIMENTAL RESULTS

Trajectory tracking is a fundamental requirement of rehabilitation robots. To verify the applicability of the PAM-based robot in rehabilitation, human gait patterns are used as reference signals. The trajectory of the hip and knee joints was collected and edited according to experimental data in Winter's textbook [22]. The amplitudes of the reference signals are 17° and 25° for the hip and knee joints, respectively. Two frequencies of 0.2Hz and 0.3Hz equivalent to about 1.0 and 1.5 km/h of treadmill speed are chosen in the experiments. The signals are collected and processed through a 6Hz low-pass filter. Based on the trials and errors method, the parameters of the ADRC controller used in the experimental system are shown in Table 2.

Table 2 ADRC parameters

Parameters	Hip articular	Knee articular
b_0	7.178	9.009
$T_{set}^{2\%}$	2.5	1.8
s^{ESO}/s_{CL}	4	5

Figure 5 and Figure 6 show experiment results when the robot tracks the 0.2Hz and 0.3Hz gait patterns. The ADRC controller achieves good performance with the deviation of the measured joint angles from their desired trajectories less than $1.0°$ for both hip and knee joints.

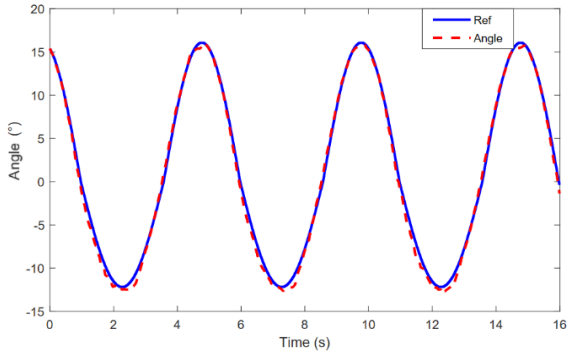

a) Hip joint

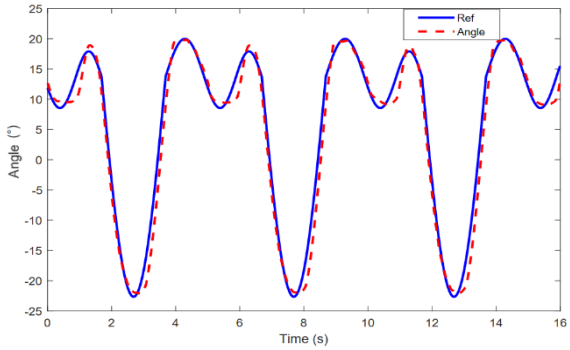

b) Knee joint

Figure 5. Trajectories of (a) hip and (b) knee joints when tracking a 0.2Hz gait pattern.

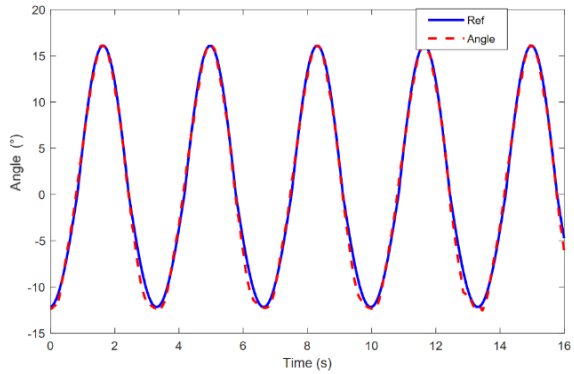

a) Hip joint

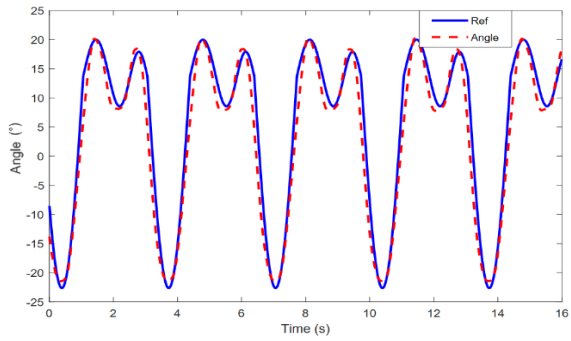

b) Knee joint

Figure 6. Trajectories of (a) hip and (b) knee joints when tracking a 0.3Hz gait pattern.

Figure 7 and Figure 8 show the estimated values of the observer together with its state variables when the robot tracks the 0.2Hz reference signal. As we can see, the observed variables z_1 is almost coincide with the output tracking trajectory x_1. The other observed variables z_2 and z_3 are also converged to their state ones. The observer can well approximate the total disturbance f.

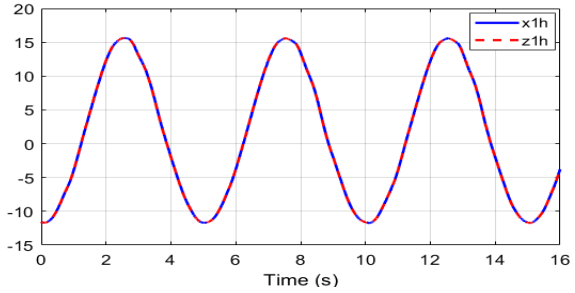

a) x_1 and z_1.

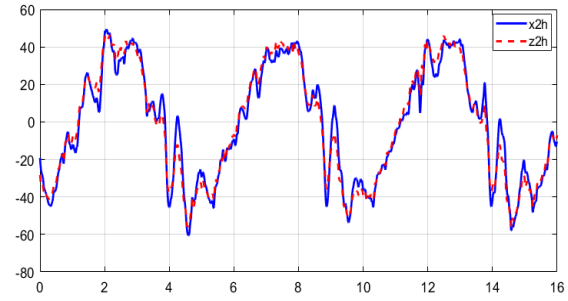

b) x_2 and z_2.

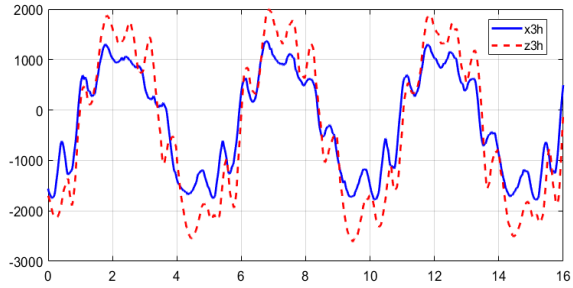

c) f and z_3.

Figure 7. State variables and its estimated values of the hip joint when the robot tracks the 0.2Hz reference signal: (a) x_1 and z_1, (b) x_2 and z_2, f and z_3.

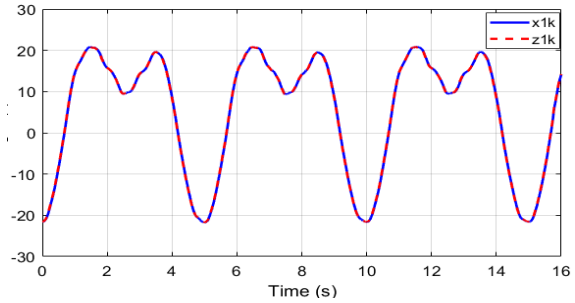

a) x_1 and z_1.

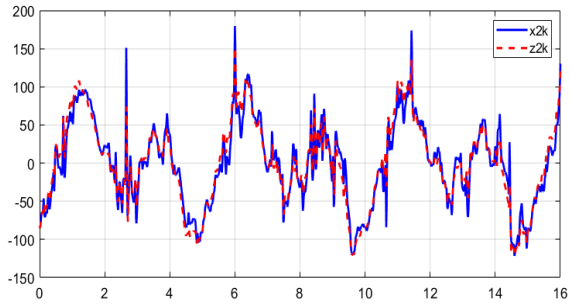

b) x_2 and z_2.

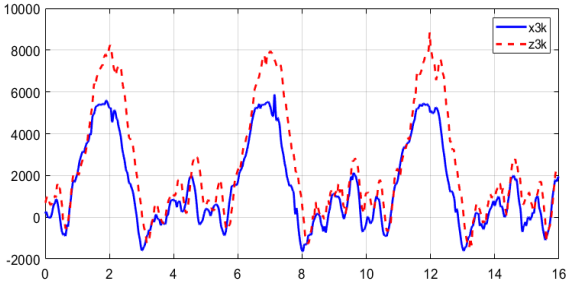

c) f and z_3.

Figure 8. State variables and its estimated values of the knee joint when the robot tracks the 0.2Hz reference signal (a) x_1 and z_1, (b) x_2 and z_2, f and z_3.

To evaluate the robustness of the control system, we conduct experiments with added load and noise conditions. The load is a 3kg weight that is rigidly attached to the system. System noise is a pulse signal whose amplitude is equal to the control signal but in reverse and is fed into the system for 0.5 seconds. Figure 9 shows the experimental results of the muscular system following the hip and knee trajectories with a 3kg load at 0.2Hz compared with the case of no load. In the experiments, the controller gives quite good results with root mean square tracking error (RMSTE) is under $2.5°$. When there is a load, the control performance of the system is slightly decreased. The deviation between the desired trajectories and the measured one of the system increases, especially in the area of low pressure. However, the system is still stable and has good tracking precision. Figure 10 presents the experimental results of the system with input disturbance. It can be seen that the system quickly returns to track desired trajectories and causes no instability. It can be concluded that with the ADRC controller the system is not only stable with an external load but also robust with uncertain disturbances of the system. Table 3 provides the RMSTE values under different experimental conditions.

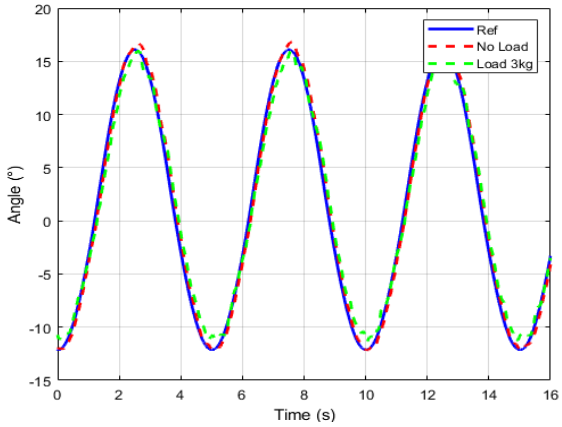

a) Hip joint's trajectory.

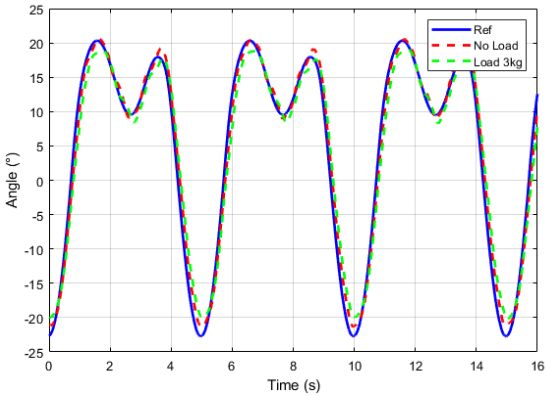

b) Knee joint's trajectory.

Figure 9. Comparison of trajectory tracking control under various conditions (load and no load) at the frequency of 0.2Hz.

Table 3. RMSTE (°) of the robot when tracking a sinusoidal signal.

Experimental condition	Hip joint		Knee joint	
	0.2Hz	0.3Hz	0.2Hz	0.3Hz
No load	0.5	0.6	0.9	1.1
3kg of load	1.1	1.3	2.1	2.2

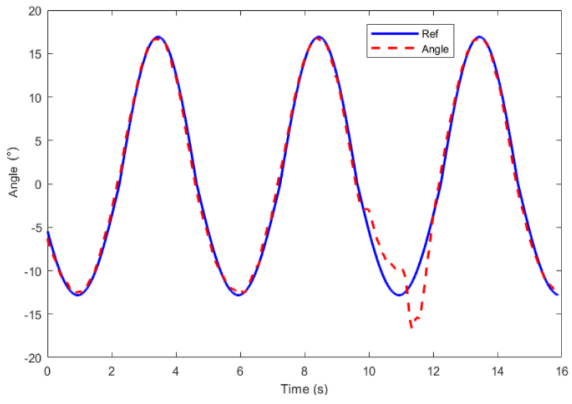

a) Frequency 0.2Hz

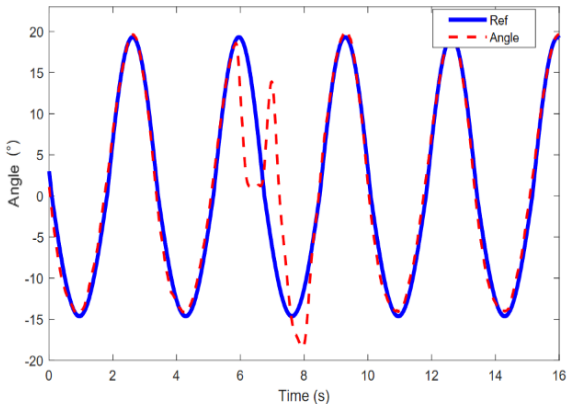

b) Frequency 0.3Hz

Figure 10. The system responds to disturbance of the hip joints when tracking the (a) 0.2Hz and (b) 0.3Hz reference signals.

6.0 CONCLUSION

In this paper, a prototype exoskeletal robot for lower-limb rehabilitation named BK-Gait is designed. The robot is powered by PAMs, soft, highly compliant actuators. The ADRC controller is employed to test the robot's trajectory tracking function. Although the maximum angle of the knee joint is about 25° because of the mechanical limitation, the experiment results when tracking a human gait pattern in multi scenarios show that the robot performs a promising application in rehabilitation. In addition, the model deviation when assuming the rod mechanism equivalent to the pulley is also compensated by the ESO. However, the frequency of the reference signal is 0.3Hz, which is relatively low compared to regular walking speed and needs improvement. Besides, the experiments are carried out without a participant of any subject. As a result, no clinical evaluation can be obtained. Both the mechanical design and control strategy of the robot must be implemented in future works to improve tracking performance. The impedance control function will also be integrated into the robot for assist-as-need training purposes.

Acknowledgement

This research is funded by Hanoi University of Science and Technology (HUST) under project number T2022 - PC - 002.

References

[1] D.W. Repperger, D.B. Reynolds, C.A. Phillips and G. Bandry. 2003. Modeling the dynamic characteristics of pneumatic muscle, *Annals of Biomedical Engineering*, 31: 310–317. DOI : https://doi.org/10.1114/1.1554921

[2] Ling Zhao, Haiyan Cheng, Yuanqing Xia and Bo Liu. 2018. Angle Tracking Adaptive Backstepping Control for a Mechanism of Pneumatic Muscle Actuators via an AESO, *IEEE Transactions on Control Systems Technology*, 66(6): 4566-4576. DOI : http://doi.org/10.1109/TIE.2018.2860527

[3] Xie, D.; Ma, Z.; Liu, J.; Zuo, S. 2021, Pneumatic Artificial Muscle Based on Novel Winding Method. Actuators 10 : 100. DOI : https://doi.org/10.3390/act10050100

[4] Hee Doo Yang, Brandyn T. Greczek and Alan T. Asbeck, 2019.Modeling and Analysis of a High-Displacement Pneumatic Artificial Muscle With Integrated Sensing, *Original Research Article*, 5(136): 1-13?DOI: http://doi.org/ 10.3389/frobt.2018.00136

[5] Mižáková J, Piteľ J, Tóthová M. 2013;Pneumatic Artificial Muscle as Actuator in *Mechatronic System. AMM* 460: 81–90. DOI : http://doi.org/ 10.4028/www.scientific.net/AMM.460.81

[6] Andrikopoulos, G.; Nikolakopoulos, G.; Manesis, S. 2014Advanced Nonlinear PID-Based Antagonistic Control for Pneumatic Muscle Actuators. *IEEE Trans. Ind. Electron.*, 61: 6926–6937 DOI: http://doi.org/ 10.1109/TIE.2014.2316255

[7] Nguyen Ngoc Son, Cao Van Kien, Ho Pham Huy Anh. 2017. A novel adaptive feed-forward-PID controller of a SCARA parallel robot using pneumatic artificial muscle actuator based on neural network and modified differential evolution algorithm. *Robotics and Autonomous Systems*, 96: 65-80, ISSN 0921-8890. DOI: http://doi.org/ 10.1016/j.robot.2017.06.012

[8] Ting Wang, Xiuxiang Chen and Wen Qin. 2019. A novel adaptive control for reaching movements of an anthropomorphic armdriven by pneumatic artificial muscles. *Applied Soft Computing*, 83: 105623. DOI : http://doi.org/10.1016/j.asoc.2019.105623

[9] J. H. Lilly and Liang Yang. 2005. Sliding mode tracking for pneumatic muscle actuators in opposing pair configuration. *in IEEE Transactions on Control Systems Technology*, 13(4): 550-558. DOI : http://doi.org/ 10.1109/TCST.2005.847333

[10] A. Enzevaee, A. Enzevaee, M. Mailah M. Mailah, and S. Kazi S. Kazi. 2018. Control Of A Single Link Robot Arm Actuated By Pneumatic Artificial Muscles Employing Active Force Control And Fuzzy Logic Via Hardware-In-The-Loop-Simulation. *Jurnal Mekanikal* 36 (2): 66-85

[11] Dao, Q.-T.; Nguyen, M.-L.; Yamamoto, S.-i. 2019. Discrete-Time Fractional Order Integral Sliding Mode Control of an Antagonistic Actuator Driven by Pneumatic Artificial Muscles. *Applied Sciences*, 9: 2503. DOI : http://doi.org/ 10.3390/app912250

[12] L. Zhao, Q. Li, B. Liu and H. Cheng, 2019"Trajectory Tracking Control of a One Degree of Freedom Manipulator Based on a Switched Sliding Mode Controller With a Novel Extended State Observer Framework," *in IEEE Transactions on Systems, Man, and Cybernetics: Systems*, 49(6): 1110-1118. DOI : http://doi.org/ 10.1109/TSMC.2017.2719057

[13] T. Choi, B. Choi and K. Seo, 2011. "Position and Compliance Control of a Pneumatic Muscle Actuated Manipulator for Enhanced Safety," in *IEEE Transactions on Control Systems Technology*, 19(4): 832-842. DOI : http://doi.org/10.1109/TCST.2010.2052362

[14] Dao Q-T, Yamamoto S-i. 2018. Assist-as-Needed Control of a Robotic Orthosis Actuated by Pneumatic Artificial Muscle for Gait Rehabilitation. *Applied Sciences.* 8(4):499. DOI : http://doi.org/10.3390/app8040499

[15] Ling Zhao, Xin Liu and TaoWang, 2019. "Trajectory tracking control for double-joint manipulator systems driven by pneumatic artificial muscles based on a nonlinear extended state observer", *Mechanical Systems and Signal Processing*, 122: 307-32. DOI : http://doi.org/10.1016/j.ymssp.2018.12.016

[16] Dao, QT., Le Tri, TK., Nguyen, VA. et al. 2022. Discrete-time sliding mode control with power rate exponential reaching law of a pneumatic artificial muscle system. *Control Theory Technol.* DOI : https://doi.org/10.1007/s11768-022-00117-8.

[17] Y. Yuan, Y. Yu, Z. Wang and L. Guo, 2019. "A Sampled-Data Approach to Nonlinear ESO-Based Active Disturbance Rejection Control for Pneumatic Muscle Actuator Systems with Actuator Saturations", *IEEE Transactions on Industrial Electronics*, 66(6): 4608-4617. DOI : http://doi.org/ 10.1109/TIE.2018.2864711

[18] Y. Yuan, Y. Yu, Z. Wang and L. Guo, 2019 "A Sampled-Data Approach to Nonlinear ESO-Based Active Disturbance Rejection Control for Pneumatic Muscle Actuator Systems with Actuator Saturations," in *IEEE Transactions on Industrial Electronics*, 66(6): 4608-4617. DOI : http://doi.org/10.1109/TIE.2018.2864711

[19] Aole S, Elamvazuthi I, Waghmare L, Patre B, Meriaudeau F. 2020. Improved Active Disturbance Rejection Control for Trajectory Tracking Control of Lower Limb Robotic Rehabilitation Exoskeleton. *Sensors*.; 20(13):3681. DOI : http://doi.org/10.3390/s20133681

[20] J. Han, 2009."From PID to Active Disturbance Rejection Control," *in IEEE Transactions on Industrial Electronics*, 56(3): 900-906. DOI : http://doi.org/ 10.1109/TIE.2008.2011621

[21] Herbst, Gernot. 2013. "A Simulative Study on Active Disturbance Rejection Control (ADRC) as a Control Tool for Practitioners" Electronics 2(3): 246-279. DOI : http://doi.org/10.3390/electronics2030246

[22] David A. Winter, 1990. “Biomechanics and Motor Control of Human Movement”, *Fourth Edition* DOI: http://doi.org/10.1002/9780470549148